

# HIGH ENERGY GAMMA RAY RESPONSE OF LIQUID SCINTILLATOR

N. SHIGYO, K. ISHIBASHI, N. MATSUFUJI and T. NAKAMOTO

*Department of Nuclear Engineering, Kyushu University  
Hakozaki, Fukuoka-shii, 812, Japan*

M. NUMAJIRI

*National Laboratory for High Energy Physics  
Oho, Tsukuba-shi, Ibaraki-ken, 305, Japan*

## Abstract

We made the experiment on the spallation reaction. NE213 organic liquid scintillators were used for measuring neutrons and  $\gamma$  rays. To produce the  $\gamma$  ray emission cross section, we used the response functions by EGS4 code. The response functions look like uniform above  $\gamma$  ray energies of 60 MeV. The experimental data of the  $\gamma$  ray emission cross section are different from the data of High Energy Transport Code.

## 1. Introduction

The NE213 scintillator which is used in the measurement of high energy neutrons is sensitive to the  $\gamma$  ray. When a flight path is short in the time-of-flight (TOF) measurement of neutrons, it is important to discriminate between neutrons and  $\gamma$  rays. If the two types of particles can be separated clearly, the cross section of the  $\gamma$  ray emission will be obtained. In this work, we obtain the response function of  $\gamma$  rays by EGS4 code, to produce the cross section of the  $\gamma$  ray creation [1].

High Energy Transport Code (HETC) [2] is used to calculate the high energy transport phenomena. The emission of the  $\gamma$  ray is considered in the some version of HETC. However, such code considers only  $\gamma$  rays from the residual nuclei after the spallation reaction. If  $\gamma$  rays from the spallation reaction are obtained, information on the other processes may be found.

## 2. Experiment on Spallation Reaction

We made the experiment on the spallation reaction at p2 beam line of 12 GeV proton synchrotron accelerator at National Laboratory for High Energy Physics (KEK). The incident proton energies were 0.8, 1.5, 3.0 GeV. The target nuclei were C, Al, Fe, In and

Pb. The emission angles in the measurement were 15, 30, 60, 90, 120 and 150 degrees. Fig. 1 shows the layout of the detectors and the target.

Since this measurement was carried out for a main purpose of obtaining the neutron emission double differential cross section, NE213 liquid organic scintillators were used for measuring neutrons and  $\gamma$  rays. The two types of scintillators were utilized in the experiment. The large ones have a diameter of 5 inch and a length of 5 inch for the priority of the detection efficiency. The others are the small size detectors which have a diameter of 2 inch and a length of 2 inch for the priority of the neutron- $\gamma$  discrimination in a low energy range. To remove the charged particles from the data, the plastic scintillator NE102A were set as veto detectors in front of individual detectors. To separate pions from the incident beam by TOF, two plastic scintillators, S0 and P0, were placed on the upper stream. Two plastic scintillators, P1 and P2 were put for verifying the incident beam to the target.

### 3. Data Analysis

#### 3.1 Discrimination between neutrons and $\gamma$ rays

The gate integration method [3] was adopted to make pulse-shape discrimination between neutrons and  $\gamma$  rays. This method uses the direct monopole output signal from the detector. The ratio of integral quantities between the rise part and the decay one for  $\gamma$  ray events is different from that for neutrons. Gamma rays are thus distinguished from neutrons. We recorded both the rise part and the decay part of the each ADC signal, and discriminated between  $\gamma$  rays and neutrons. Fig. 2 shows neutron- $\gamma$  discrimination.

#### 3.2 Energy calibration of detector

The ADC spectra obtained by the experiment were calibrated by the  $\gamma$  ray checking source ( $^{137}\text{Cs}$ ,  $^{60}\text{Co}$  and Am-Be). Through the calibration, it was confirmed that the ADC linearity was kept in the range of 0.5 - 4.4 MeV. We attempted to calibrate by the use of the TOF neutron energy scale above 4.4 MeV.

#### 3.3 Determination of response function

With regard to  $\gamma$  ray energy below 10 MeV, detector response functions were calculated by EGS4. Since the energy resolution of the detector is not considered by EGS4, we calculated the resolution by the following equation to obtain the actual response functions.

$$G(X) = \frac{C_x}{\sigma\sqrt{2\pi}} \exp \left[ -\frac{(X - X_0)^2}{2\sigma^2} \right], \quad (5)$$

where  $\sigma^2$  is the deviation,  $X_0$  is the peak channel,  $C_x$  is the counts of the peak channel,

and  $G(X)$  is the counts of the channel  $X$ .

On the basis of the energy resolution, we got the actual response functions considering the energy resolution of the detectors by  $G(X)$  and the response functions calculated by EGS4.

$$R_{ri} = \sum G_{ij} R_j. \quad (6)$$

Figure 3 shows the response functions on the condition that the  $\gamma$  ray energy is 1.25 MeV and the energy resolutions range from 0 % to 30 %. Fig. 4 indicates the comparison of the spectra of a  $^{60}\text{Co}$  standard checking source and the response function in the case that the energy resolution is 25 %.

In addition, we also calculated the detector response functions for high energy  $\gamma$  rays by EGS4. In order to fit the condition of the experiment, the detector geometry for EGS4 was determined as shown Fig. 5. This calculation assumed that the  $\gamma$  ray source was 1 m apart from the scintillator front plane, and  $\gamma$  rays were emitted radiately from the point source.

Figures 6 and 7 indicate the calculation results by EGS4. When the  $\gamma$  ray energy is close to 20 MeV, the sharp peak appears 0.5 MeV below its energy. Above 40 MeV, the Compton edge is not seen. The response functions look like almost uniform above 60 MeV.

### 3.4 Determination of detection efficiency

In this work, the detection efficiencies for  $\gamma$  rays were determined by the response function with EGS4. Fig. 8 indicates the detection efficiency. Since the function is given in units of count/MeV/incidence, the integral values of each channel of the response function correspond to the detection efficiency.

## 4. Preliminary Analysis of Cross Section

To obtain the cross section of the  $\gamma$  ray emission, we used FERDO code [4].  $\gamma$  rays above 10 MeV were ignored in the preliminary analysis. Fig. 9 shows the double differential cross section of the  $\gamma$  ray emission from the spallation reaction. The marks are the experimental data, and the lines are the calculation results by HETC-KFA2 [5] code. The experimental data are lower than the data of HETC-KFA2 in all angle. In the experiment, only the prompt  $\gamma$  rays ( $< 3$  ns) were taken to ADC. However, HETC-KFA2 only considers that  $\gamma$  rays are emitted from nuclei after delay.

## 5. Conclusion

Gamma rays from the spallation reaction were measured by the use of NE213 scintillator. By the gate integration method, the neutron and the  $\gamma$  ray up to 70 MeV was discriminated. The response functions by EGS 4 were obtained and showed a uniform distribution above  $\gamma$  ray energies of 60 MeV.

## Acknowledgment

We express their gratitude to Prof. H. Hirayama, Dr. S. Ban and Dr. Y. Namito of National Laboratory for High Energy Physics for useful suggestion and discussion.

## References

- [1] W. R. Nelson, et al., *The EGS4 Code System* SLAC-Report-265 (1985).
- [2] K. C. Chandler and T. W. Armstrong, *ORNL-Report 4744* (1972).
- [3] F. D. Brools, *Nucl. Instrum. Meth.*, 4, 151 (1959).
- [4] W. R. Burrus, *ORNL-Report 3743* (1965).
- [5] R. E. Prael and H. Lichtenstein, *LA-UR 89-3014*, 45 (1989) Cambridge University Press, 1990.

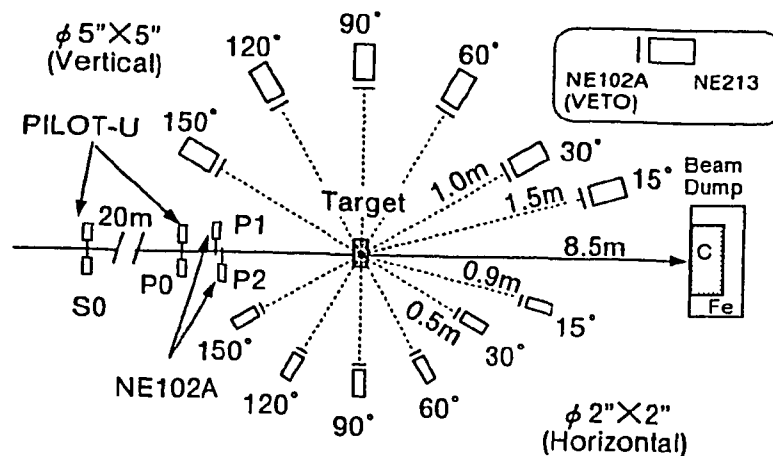


Fig. 1 Layout of detectors and target

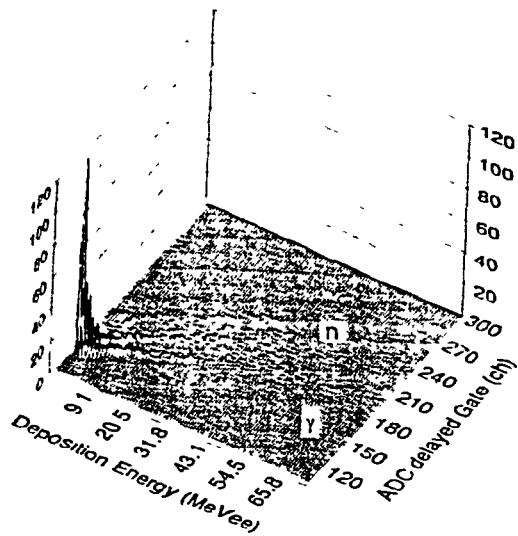


Fig. 2 neutron-gamma discrimination by gate integration method  
800 MeV p on In,  $\Phi$  5" x 1 5" detector on 15°

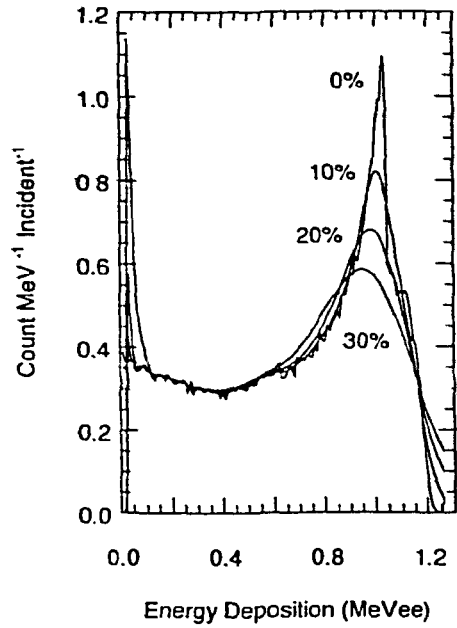


Fig. 3 Effect of energy resolution for 1.25 MeV  $\gamma$  ray response function

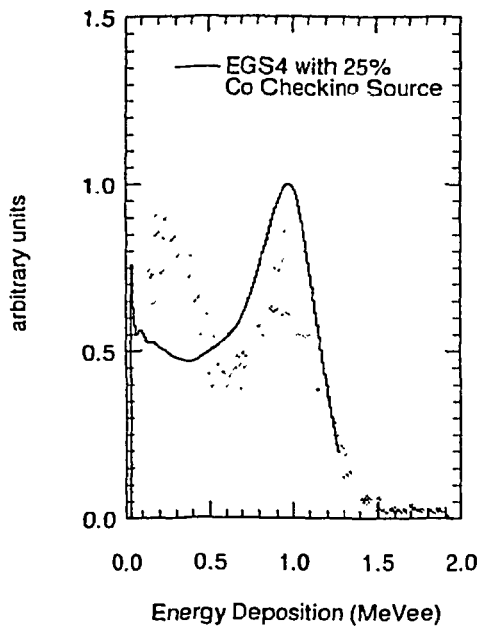


Fig. 4 Comparison of response function by EGS 4 and  $^{60}\text{Co}$  checking source

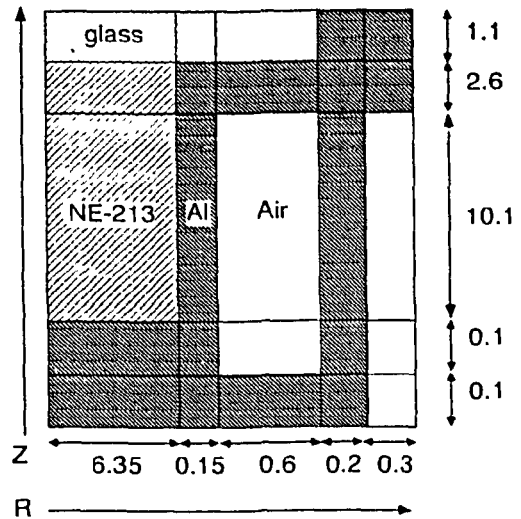


Fig. 5 Detector geometry

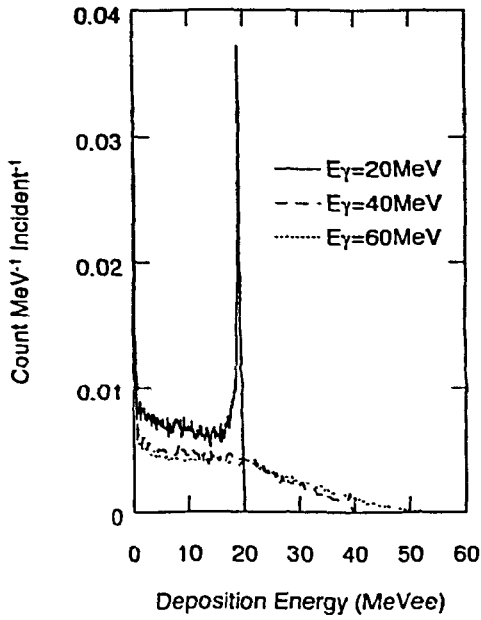


Fig. 6 Response function by EGS 4 for 20, 40, 60 MeV  $\gamma$  ray

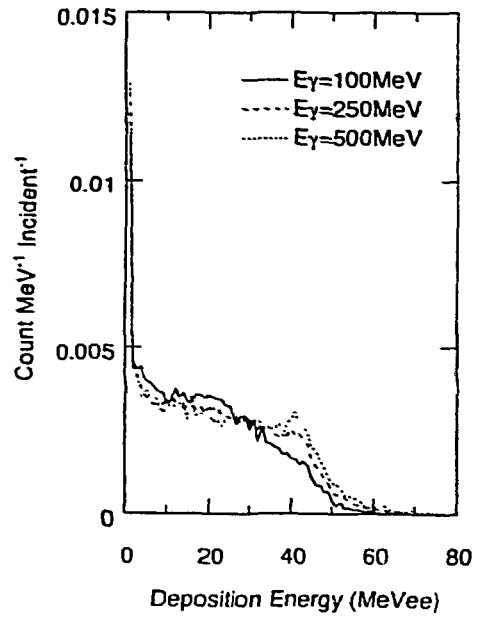


Fig. 7 Response function by EGS 4 for 100, 250, 500 MeV  $\gamma$  ray

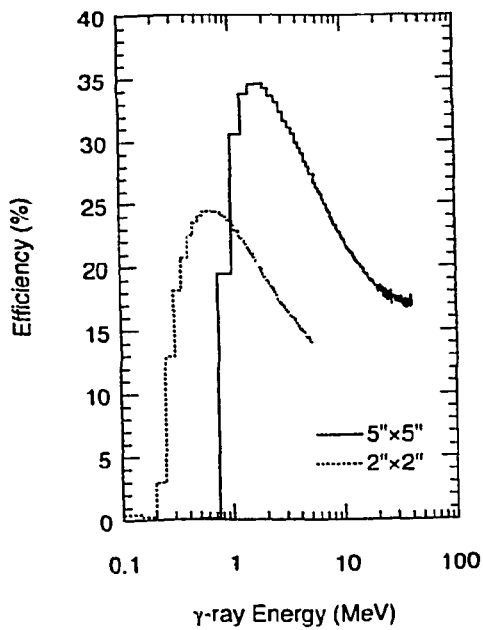


Fig. 8 Detection efficiency by EGS 4

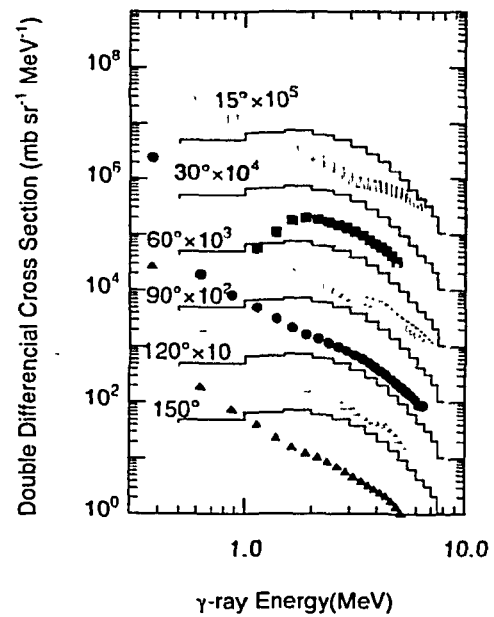


Fig. 9  $\gamma$  ray creation double differential cross section for 1.5 GeV p on In